Turkish Journal of Electrical Engineering & Computer Sciences

http://journals.tubitak.gov.tr/elektrik/

Research Article

Turk J Elec Eng & Comp Sci
(2020) 28: 2213 – 2227

doi:10.3906/elk-1912-34

Disturbance observer based control of twin rotor aerodynamic system

Hamid ALI*, **Ahsan ALI**, **Inam Ul Hasan SHAIKH**
Electrical Engineering Department, University of Engineering and Technology Taxila, Taxila, Pakistan

Received: 04.12.2019 • **Accepted/Published Online:** 03.04.2020 • **Final Version:** 29.07.2020

Abstract: Twin rotor aerodynamic system (TRAS) approximates the dynamics of helicopters and other vertical take off rotor crafts. The nonlinear nature with significant cross-coupling between the inputs and outputs of the main and tail rotors make the control of such system for either stabilization or reference tracking a challenging task. In this paper, the problem of disturbance rejection for TRAS is addressed by designing disturbance observers through H_∞ based approach. The system is decoupled into main and tail rotors subsystems. For each subsystem, an inner loop disturbance observer is synthesized that provides disturbance rejection, whereas to ensure stability and performance an outer loop baseline feedback controller is designed. Two different cases are considered. In first case 2 proportional-integral-derivative controllers are designed to use as outer loop baseline feedback controllers with disturbance observers whereas in the second case linear quadratic Gaussian (LQG) controllers are designed. For both cases simulations are performed with nonlinear Matlab Simulink model of TRAS and results are compared to determine which approach delivers better performance. Simulation results show that the 2 conflicting requirements of reference tracking and disturbance rejection can be met simultaneously with the proposed approach increasing the disturbance rejection capability of the closed loop system.

Key words: Disturbance observer, twin rotor aerodynamic system, H_∞ approach, optimal control, decoupling

1. Introduction

In recent years, many novel concepts and advanced techniques are introduced in aircraft design and control of aerodynamic systems. These techniques and concepts are different in configurations and control structures from their predecessors. Aerodynamic systems such as unmanned aerial vehicles and helicopters offer several advantages for surveillance, rescue operations and inspection tasks because they can land, hover and take off vertically in narrow environments and confined spaces. Still, since these systems consist of rotors for which the control inputs are aerodynamic forces and torques produced by these rotors, controllers design for such systems with complicated system dynamics is a difficult task. In addition, a strong cross-coupling between different rotors in these dynamic systems increases the nonlinearities and uncertainties [1]. These characteristics introduce rigorous challenges to the controller design for such systems [2, 3].

A model of a helicopter, usually termed as twin rotor aerodynamic system (TRAS) is generally used in research labs for testing the effectiveness and performance of controllers designed for helicopters and unmanned aerial systems. TRAS consists of a beam on which 2 rotors, called the main and the tail rotors are mounted. The main objective of controller design for TRAS is to control the main and tail rotors so that some desired trajectory of pitch and yaw angles is tracked while rejecting disturbances. The complications in controller design for TRAS originates from nonlinearity and cross-coupling between the main and tail rotors. To design

*Correspondence: engr.hamidali94@gmail.com

controllers for this system we first need a mathematical model of TRAS. In [4, 5], the nonlinear differential equations are obtained for TRAS. These equations are linearized and converted to state space model. In [6], data obtained from a real laboratory model is used to experimentally identify the nonlinear model of the TRAS.

Intelligent computational techniques like neural networks, fuzzy systems and genetic algorithms that are mostly used in literature are utilized successfully to obtain solution of control problems for the last few years. In [7], the fuzzy logic and PID control techniques are combined to make a hybrid fuzzy-PID-based controller. This controller shows excellent control and tracking capability. However, disturbance rejection or robustness is not discussed.

Usually, both the reference tracking and disturbance rejection are desirable in the control design of systems like TRAS. H_∞ controller is a frequency domain technique that provides robustness and has disturbance rejection capability. It was first proposed by Zames in 1981 [8]. In [9] an optimal and robust model predictive controller (MPC) is designed for TRAS and it is shown that MPC has minimum settling and rise time as compared to linear quadratic regulator (LQR). Although MPC is a powerful technique used for controlling the multi variable systems however it requires accurate mathematical models and also since a large number of parameters to be tuned by the user it is the most time consuming method [10]. For both disturbance rejection and reference tracking, many times 2 degree of freedom (DOF) controllers are used. In [11], a 2 DOF robust controller is designed for DC servomotors that provides trajectory tracking. Two DOF H_∞ controllers are designed in [12, 13], that provide robustness as well as reference tracking.

In [14], a stabilizing control law is presented where a nonlinear observer is utilized to predict the states. TRAS model is decoupled and decomposed into 2 subsystems. The coupling effect between the subsystems in this case is considered as the uncertainties and chattering effect found in the control signal is reduced without degrading the tracking performance. In [15], a method is presented to obtain robust stability bounds for TRAS. An observer based H_∞ controller is designed and the stability is examined by using Kharitonov's theorem. It is shown that within a certain uncertainty limit, the TRAS controlled by H_∞ controller with nonlinear observer gives the stable response.

Sliding mode control techniques are broadly used in the literature for the control of dynamic systems. These controllers can be used when the input is saturated [16]. In [17], an adaptive nonlinear gain based composite controller is presented. To improve the system response, a nonlinear adaptive gain is employed in the composite controller. An adaptive law for the nonlinear gain using the Lyapunov theory is developed. The results of this technique shows improved reference tracking, however the robustness margin is very small.

In disturbance observer (DOB) based control scheme, the outer loop baseline feedback controller is designed for reference tracking and stability, whereas the inner loop DOB is designed to estimate and reject disturbances and suppress uncertainty [18]. Under no disturbance condition, the inner loop which estimates and compensates the disturbances is not active. The 2 conflicting requirements of disturbance rejection and reference tracking can be met by separately designing the outer loop baseline feedback controller and the inner disturbance rejection loop. This distinguishes DOB based control scheme from some other control techniques. For example, to improve the robustness and disturbance rejection in traditional PID controller the integral action is introduced in it. But, by doing so percent overshoot is also increased and stability of the system is degraded. Furthermore, unlike DOB based control scheme in most robust control approaches the nominal performance is compromised to acquire better robustness and are termed as the worst case based design.

In this paper, a DOB based control scheme is employed for TRAS. A decoupler is designed which decouples the system into main and tail rotors subsystems. First 2 outer loop PID controllers are designed for both the

main and tail rotors so that the pitch and yaw angles of TRAS are controlled. After designing the PID controllers, disturbance observers are designed. The results obtained in both cases i.e. with and without using the DOB, with PID controller in the outer loop are then compared. This process is repeated for LQG controller as baseline feedback controller in the outer loop. Results obtained for LQG controllers with DOB are compared with PID controller with DOB. In section 2, the mathematical modelling and the state space representation of TRAS is presented. In section 3, decoupler is designed to decouple TRAS into main and tail rotor. In section 4, procedure for H_∞ based observer design is presented. In section 5 baseline feedback controllers are designed. Simulation results are discussed in section 6 followed by conclusion in section 7.

2. Mathematical modelling of TRAS

The sketch of TRAS which we are using in this paper is shown in Figure 1. The speed of rotation of main rotor affects the aerodynamic forces, torques and the pitch angle of main rotor while the speed of rotation of tail rotor controls the aerodynamic forces, torques and the yaw angle of tail rotor. The speed of rotation is controlled by magnitude of voltage of the main and tail motors.

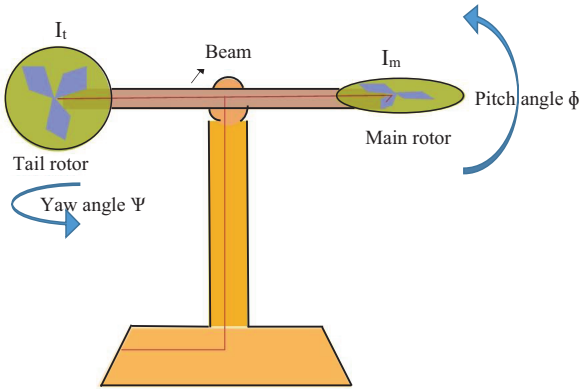

Figure 1. Twin rotor aerodynamic system.

The dynamics of TRAS as presented in [19–21] are used in this paper. The parameters used in the equations that follow are given in Table 1. The momentum equation for the main rotor (pitch angle) is given by

$$I_m\ddot{\psi} = M_m - M_{FF} - M_{B\psi} - M_G, \tag{1}$$

where M_m is the main rotor's gross momentum, $M_{B\psi}$ is friction forces momentum, M_{FF} is the gravity momentum and M_G is gyroscopic momentum. These momentums are given by the following equations:

$$M_m = a_1\tau_1^2 + b_1\tau_1$$

$$M_{B\psi} = B_{1\psi}\dot{\psi} - B_{2\psi}sin(2\psi)\dot{\phi}^2$$

$$M_{FF} = M_g sin\psi$$

$$M_G = K_{gy}M_m\dot{\phi}cos\psi$$

Table 1. Parameters of the TRAS laboratory model [20].

Parameters	Description	Value
T_0	Cross-coupling momentum constant	3.5
I_m	Inertia of main rotor	0.068 kgm^2
a_1	Constant	0.0135
T_P	Cross-coupling momentum constant	2
I_t	Inertia of tail rotor	0.02 kgm^2
a_2	Constant	0.02
b_1	Static parameter	0.0924
$B_{2\psi}$	Friction constant	0.001 Nms^2/rad
b_2	Static parameter	0.09
M_g	Gravity constant	0.32 Nm
$B_{1\psi}$	Friction constant	0.006 Nms/rad
K_2	Tail rotor's motor gain	0.8
$B_{1\phi}$	Friction constant	0.1 Nms/rad
T_{21}	Tail rotor's constant	1
K_{gy}	Gyroscopic momentum	0.05 s/rad
K_1	Main rotor's motor gain	1.1
$B_{2\phi}$	Friction constant	0.01 Nms^2/rad
T_{11}	Main rotor's constant	1.1
T_{10}	Main rotor's constant	1
T_{20}	Tail rotor's constant	1
K_0	Cross-coupling momentum gain	-0.2

The relationship between main rotor's input voltage u_1 and torque produced τ_1 is given by the transfer function

$$\tau_1 = \frac{K_1}{T_{11}s + T_{10}} u_1. \tag{2}$$

Similarly the momentum equation for tail rotor (yaw angle) is given by

$$I_t\ddot{\phi} = M_t - M_{B\phi} - M_{CR}, \tag{3}$$

where M_t is the tail rotor's gross momentum, $M_{B\phi}$ is friction forces momentum and M_{CR} is approximate cross-reaction momentum. These momentums are given by

$$M_t = a_2\tau_2^2 + b_2\tau_2,$$

$$M_{B\phi} = B_{1\phi}\dot{\phi},$$

$$M_{CR} = \frac{K_c(T_0 s + 1)}{T_p s + 1} M_m.$$

The relationship between tail rotor's input voltage u_2 and torque produced τ_2 is given by the transfer function

$$\tau_2 = \frac{K_2}{T_{21}s + T_{20}} u_2. \tag{4}$$

The nonlinear equations (1-4) are linearized by selecting the operating point as $[\phi, \psi] = [0, 0]$, and the output and state vectors are selected as $y = [\phi, \psi]^T$ and $x = [\tau_1, \phi, \dot{\phi}, \tau_2, \psi, \dot{\psi}, M_{CR}]^T$, respectively.

Where ψ is yaw angle, $\dot{\psi}$ is yaw velocity, ϕ is pitch angle and $\dot{\phi}$ is pitch velocity. After linearization the following state space matrices are obtained:

$$A = \begin{bmatrix} -0.833 & 0 & 0 & 0 & 0 & 0 & 0 \\ 0 & 0 & 1 & 0 & 0 & 0 & 0 \\ 1.246 & -4.706 & -0.0883 & 0 & 0 & 0 & 0 \\ 0 & 0 & 0 & -1 & 0 & 0 & 0 \\ 0 & 0 & 0 & 0 & 0 & 1 & 0 \\ 1.482 & 0 & 0 & 3.6 & 0 & -5 & 18.75 \\ -0.0169 & 0 & 0 & 0 & 0 & 0 & -0.5 \end{bmatrix},$$

$$B = \begin{bmatrix} 1 & 0 & 0 & 0 & 0 & 0 & 0 \\ 0 & 0 & 0 & 1 & 0 & 0 & 0 \end{bmatrix}^T,$$

$$C = \begin{bmatrix} 0 & 1 & 0 & 0 & 0 & 0 & 0 \\ 0 & 0 & 0 & 0 & 1 & 0 & 0 \end{bmatrix},$$

and

$$D = \begin{bmatrix} 0 & 0 \\ 0 & 0 \end{bmatrix}.$$

This model is used later in this work for controller design.

3. Decoupler designs

From the state space model the transfer function matrix is obtained as

$$G(s) = \begin{bmatrix} G_{11}(s) & G_{12}(s) \\ G_{21}(s) & G_{22}(s) \end{bmatrix}, \tag{5}$$

where

$$G_{11}(s) = \frac{1.246}{s^3 + 0.922s^2 + 4.76s + 3.917},$$

$$G_{12}(s) = 0,$$

$$G_{21}(s) = \frac{1.481s + 0.4233}{s^4 + 6.34s^3 + 7.06s^2 + 2.09s},$$

$$G_{22}(s) = \frac{3.6}{s^3 + 6s^2 + 5.01s}.$$

From the transfer function matrix, it is clear that there is a strong interaction between the main rotor input u_1 and main rotor output y_1, main rotor input u_1 and tail rotor output y_2 and tail rotor input u_2

and tail rotor output y_2 while there is no interaction between tail rotor input u_2 and main rotor output y_1. Therefore this section focuses on designing of decoupler so that the interaction between u_1 and y_2 (coupling effect) is minimized. A general decoupling method given in [21] is used to obtain a decoupler for the plant. Using this method for a square plant $G(s)$, decoupler can be obtained using

$$G_D(s) = G_{inv}(s)G_R(s), \tag{6}$$

where $G_{inv}(s)$ is the inverse of the plant G(s), $G_D(s)$ is the decoupler, and $G_R(s)$ is a diagonal matrix. For $G(s)$ given in Equation 5 above

$$G_{inv}(s) = \begin{bmatrix} G_{inv_{11}}(s) & G_{inv_{12}}(s) \\ G_{inv_{21}}(s) & G_{inv_{22}}(s) \end{bmatrix},$$

where

$$G_{inv_{11}}(s) = 0.8026s^3 + 0.74s^2 + 3.82s + 3.144,$$

$$G_{inv_{12}}(s) = 0,$$

$$G_{inv_{21}}(s) = \frac{-0.3302s^7 - 2.38s^6 - 5.705s^5 - 13.69s^4 - 19.13s^3 - 10.95s^2 - 1.852s + 3.423e^{-12}}{s^4 + 6.34s^3 + 7.06s^2 + 2.09s + 4.844e^{-13}},$$

$$G_{inv_{22}}(s) = 0.278s^3 + 1.67s^2 + 1.39s.$$

The decoupled plant $G_R(s)$ considered can be given by

$$G_R(s) = \begin{bmatrix} G_m(s) & 0 \\ 0 & G_t(s) \end{bmatrix}$$

$$= \begin{bmatrix} \frac{1.246}{s^3+0.9214s^2+4.78s+3.918} & 0 \\ 0 & \frac{3.6}{s^3+6s^2+5s} \end{bmatrix}.$$

From Equation 6 the decoupling matrix obtained is

$$G_D(s) = \begin{bmatrix} G_{D_{11}}(s) & G_{D_{12}}(s) \\ G_{D_{21}}(s) & G_{D_{22}}(s) \end{bmatrix},$$

where

$$G_{D_{11}}(s) = 1, \quad G_{D_{12}}(s) = 0, \quad G_{D_{22}}(s) = 1,$$

and

$$G_{D_{21}}(s) = \frac{-0.4114s^7 - 2.965s^6 - 7.109s^5 - 17.06s^4 - 23.84s^3 - 13.64s^2 - 2.307s + 4.266e^{-12}}{s^7 + 7.262s^6 + 17.67s^5 + 42.69s^4 + 60.37s^3 + 37.6s^2 + 8.187s + 1.898e^{-12}}.$$

4. H_∞ disturbance observer design

The structure of conventional DOB for a general plant $G_2(s)$ is shown in Figure 2, where $G_2(s)$ is the real physical system, $C(s)$ is the outer loop feedback controller that is responsible for performance and stability in case there is no disturbance, $G_1(s)$ is the disturbance model, $G_n(s)$ is the model of the plant called nominal model that is used for the design of controller, $G_n^{-1}(s)$ is the inverse of nominal model and $Q(s)$ is a low pass filter the degree of which is higher than $G_n^{-1}(s)$.

The basic idea of DOB is to estimate the unknown quantities such as disturbances and uncertainties termed as disturbance estimate $\hat{d}$ from the known quantities such as control signal $\hat{u}$ and plant output $y_m(s)$. This disturbance estimate $\hat{d}$ is then filtered out by the low pass filter $Q(s)$, and is finally minimized from the controller output u. In design of DOB, the filter design is an important step because it maintains DOB's robustness and causality. Since $G_n(s)$ is always causal and proper its inverse will be improper, noncausal and not be physically realizable. Therefore, $Q(s)$ needs to be designed such that $Q(s)G_n^{-1}(s)$ is proper and causal. In addition if there exists any kind of uncertainty in the real physical system $G_2(s)$, then $Q(s)$ must be designed such that robustness of DOB is guaranteed. The relationship for the disturbance estimate $\hat{d}$ found in Figure 2 with $G_2(s) = G_1(s) = G(s)$ and $X(s) = (1 + G(s)C(s))^{-1}$ is given by [22]

$$\hat{d} = \frac{Q(s)\Big(G_n^{-1}(s)G(s) + G(s)C(s)\Big)X(s)}{\Big(1 - Q(s)\Big) + Q(s)\Big(G_n^{-1}(s)G(s) + G(s)C(s)\Big)X(s)}d. \tag{7}$$

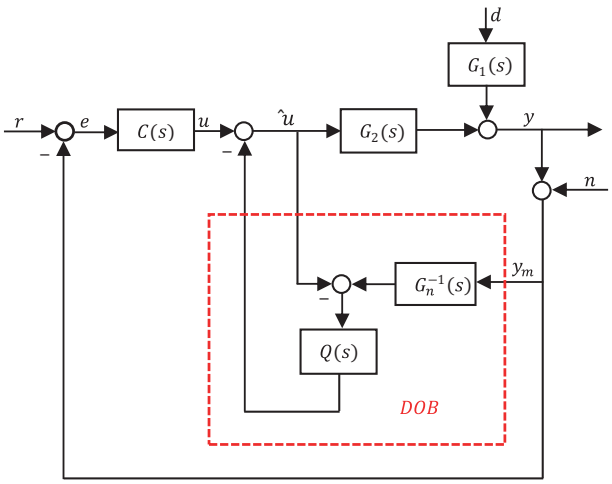

Figure 2. Structure of conventional DOB for a general system.

Now to make a perfect estimate of disturbance i.e. $\hat{d} = d$ we need to make $Q(s) = 1$ and $G^{-1}(s)G(s) = 1$ in Equation 7, which is the ideal case.

In this paper, we present H_∞ based DOB design method that is introduced in [23]. In this method, a systematic approach is utilized to find an optimal DOB that minimizes the H_∞ norm from disturbance d to its estimation error e of the weighted transfer function . The DOB design problem is then solved using linear matrix inequalities as it becomes a standard optimal H_∞ control problem. The synthesized DOB using the

above approach is guaranteed to be optimal and stable. The H_∞ based DOB structure is shown in Figure 3a which can be equivalently represented as shown in Figure 3b (assuming $Wn = Wd = 1$). Where the upper side, denoted by $P(s)$, is the generalized plant and the lower side $D(s) = [D_1(s), D_2(s)]$, is the DOB to be designed with measured output y_m and control input $\hat{u}$ as 2 inputs, and estimated disturbance $\hat{d}$ as output.

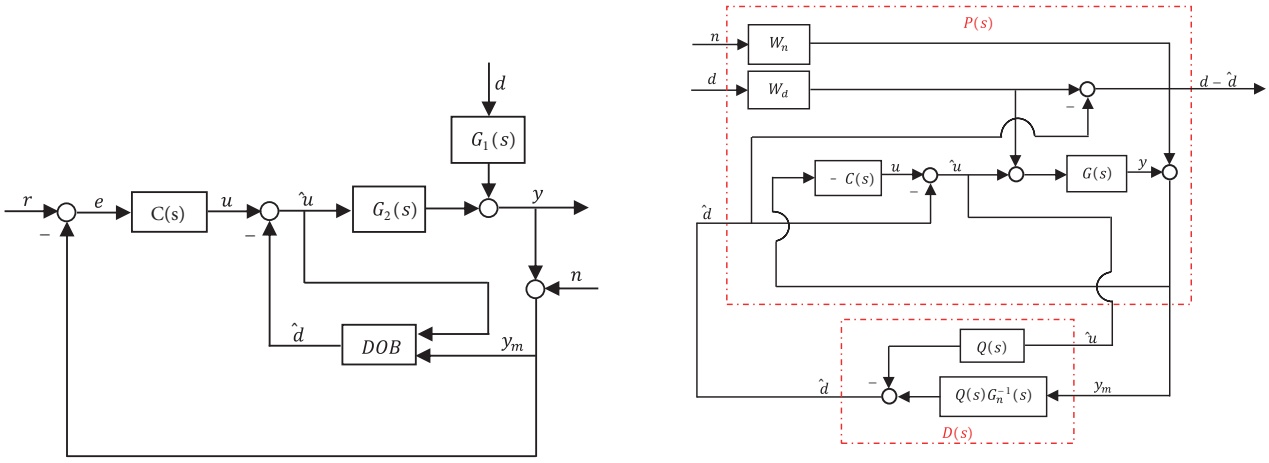

(a) H ∞ based DOB design structure

(b) Generalized plant with disturbance observer

Figure 3. H∞ based DOB design structure.

The H_∞ based DOB design approach then gives an optimal DOB $D(s)$ for partitioned plant P that minimizes the H_∞ norm from 2 external unknown inputs $[n, d]^T$ to disturbance estimation error d - $\hat{d}$ i.e.

$$\min_D \|(F_L(P, D)\|_\infty = \min_w(\max_w \bar{\sigma}(F_L(P, D)(j\omega))), \tag{8}$$

where $F_L(P, D)$ represents the lower linear fractional transform. The generalized plant P for the structure of Figure 3b, with $X = (1 + GC)^{-1}$ is obtained as

$$P(s) = \begin{bmatrix} 0 & Wn & -I \\ XW_n & XGW_d & XG \\ -CXW_n & -CXGW_d & I + CXG \end{bmatrix}.$$

Here s is omitted for simplicity. After finding the DOB $D(s)$, the Q-filter and nominal plant inverse can be reconstructed by $Q(s) = -D_1(s)$ and $G_n^{-1}(s) = -D_1(s)^{-1}D_2(s)$ respectively, to make comparison with conventional DOB.

5. Design of outer loop baseline feedback controller

In H_∞ based DOB design approach used in this paper :

a. Before the design of DOB an outer loop baseline feedback controller $C(s)$ is needed to meet performance specifications and stability as in other DOB based control schemes.

b. The DOB to be designed depends on $C(s)$.

The design of DOB in H_∞ based approach is based on generalized plant $P(s)$, and $C(s)$ is the part of the $P(s)$ as shown in Figure 3b which means H_∞ based DOB design approach depends on $C(s)$. This section briefly describes the baseline feedback controllers used for both the main and tail rotors of TRAS.

5.1. Design of PID controller

The 2 PID controllers designed for both the main and tail rotors are given by

$$G_{bm}(s) = K_{pm} + \frac{K_{im}}{s} + K_{dm}\frac{N_m}{1 + N_m\frac{1}{s}},$$

$$G_{bt}(s) = K_{pt} + \frac{K_{it}}{s} + K_{dt}\frac{N_t}{1 + N_t\frac{1}{s}},$$

where $G_{bm}(s)$ and $G_{bt}(s)$ are baseline feedback PID controllers for main and tail rotors respectively. Here K_{pm} represents the proportional gain, K_{im} the integral gain, K_{dm} the derivative gain and N_m is the filter coefficient of PID controller for main rotor, while K_{pt} represents the proportional gain, K_{it} the integral gain, K_{dt} the derivative gain and N_t is the filter coefficient of PID controller for tail rotors. The values of these quantities are given in Table 2.

Table 2. Baseline PID controllers parameters [21].

Parameters	Value	Parameters	Value
K_{pm}	0.045	K_{pt}	3.8
K_{im}	0.75	K_{it}	3.5
K_{dm}	0.35	K_{dt}	2.4

5.2. Design of LQG controller

Linear quadratic Gaussian or LQG as it is called, is an optimal observer based output feedback controller. Instead of measuring the states, output of the system is measured and states are estimated using optimal observer gains. These estimated states are then used for optimal state feedback controller. The standard LQG controller can be designed by finding an optimal control input $u(t)$ that minimizes

$$J = E[\lim_{T\to\infty}\frac{1}{T}\int_0^T [x(t)^T Q x(t) + u(t)^T R u(t)]dt], \tag{9}$$

where E is the expectation operator, $x(t)$ is the state vector, $u(t)$ is the control input and Q and R are the design parameters that must be chosen appropriately such that $Q = Q^T \geq 0$ and $R = R^T > 0$. The above is a quadratic performance index involving a linear plant, and since it also involves expectation operator E, the controller design based of this is termed in the literature as LQG controller.
To design an LQG controller it is necessary to find an optimal state feedback gain matrix K_r given by

$$K_r = R^{-1}B^T X, \tag{10}$$

where $X = X^T \geq 0$ is the unique positive semidefinite matrix obtained by solving of the algebraic Riccati equation

$$A^T X + XA - XBR^{-1}B^T X + Q = 0, \tag{11}$$

and Kalman filter gain matrix K_f given by

$$K_f = YC^T V^{-1}, \tag{12}$$

where $Y = Y^T \geq 0$ is the unique positive semidefinite matrix obtained by solving of the algebraic Riccati equation

$$YA^T + AY - YC^T V^{-1} CY + W = 0. \tag{13}$$

Using standard LQG design procedure a controller without integral action is obtained. In order to design an LQG controller that have an integral action the plant $G_2(s)$ is augmented with an integrator. Using the procedure above LQG controllers for both the main and tail rotors are designed in Matlab (Simulink) as shown in Figure 4. The Matlab (Simulink) model of subsystem TRAS is shown in Figure 5.

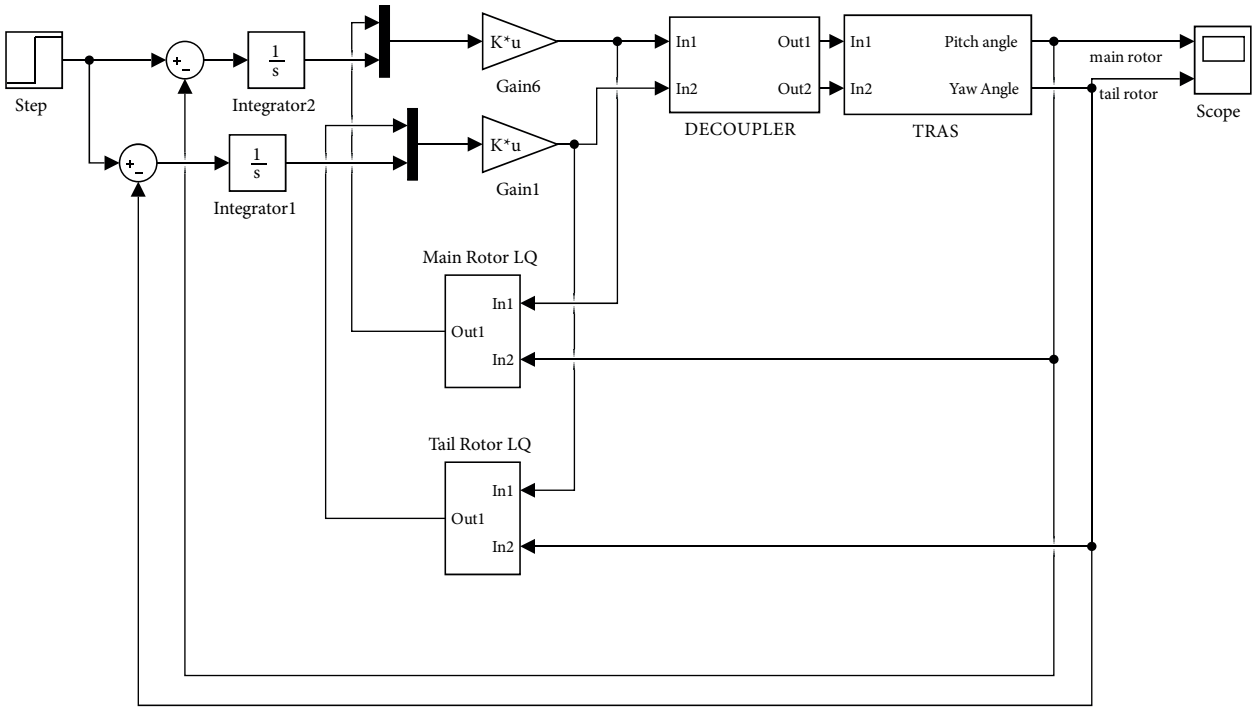

Figure 4. LQG controller designed in Matlab (Simulink).

6. Simulation results

Using the approach as given in section 4, disturbance observers are designed for both the main and tail rotors of TRAS. Two sets of simulations are performed, 1 set is for PID controllers as baseline feedback controllers and the other 1 is for LQG controllers as baseline feedback controllers.

In the first set of simulations the step responses of the main and tail rotors are shown in Figures 6a and 6b, respectively. A step disturbance is added at $t = 30$ s and its effect with and without DOB is shown. The

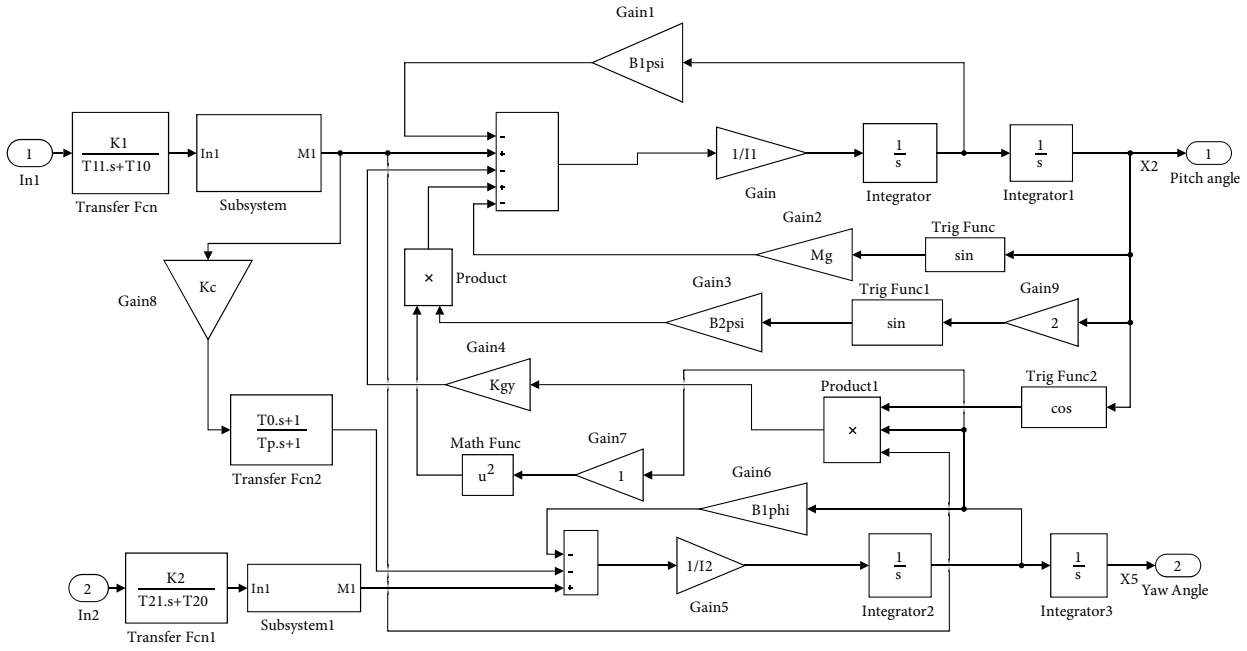

Figure 5. Matlab (Simulink) model of TRAS.

dotted lines shows the step responses of the main and tail rotors without using the DOB, whereas the solid line shows the step responses with DOB.

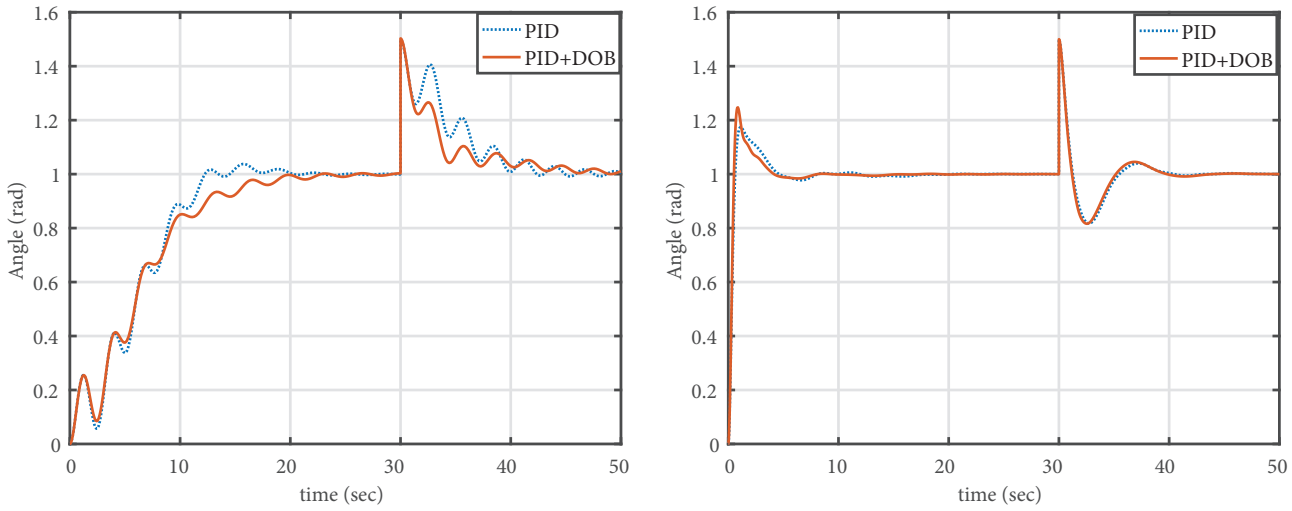

(a) main rotor (b) tail rotor

Figure 6. Response of TRAS for step input with step disturbance at t = 30s.

By observing the plots we see that when disturbance observer is used, the nominal performance specifications like rise time, settling time and overshoot are slightly affected and remained nearly the same as when disturbance observer is not used, however improvement is made in disturbance rejection. In both cases i.e. with and without DOB, the response is not smooth enough, and there are some fluctuations in the plots of main rotor,

similarly there is an overshoot in the plots of the tail rotor. It is because the nominal performance specifications depends on the outer loop baseline feedback controller. By using a good reference tracking controller with H_∞ DOB, better response can be expected.

Similarly in the second set of simulations (LQG as baseline feedback controller) the step responses of the main and tail rotors are shown in Figures 7a and 7b, respectively. A step disturbance is added at $t = 30$ s and its effect with and without DOB is shown. The dotted lines shows the step responses of the main and tail rotors without using the DOB, whereas the solid line shows the step responses with DOB.

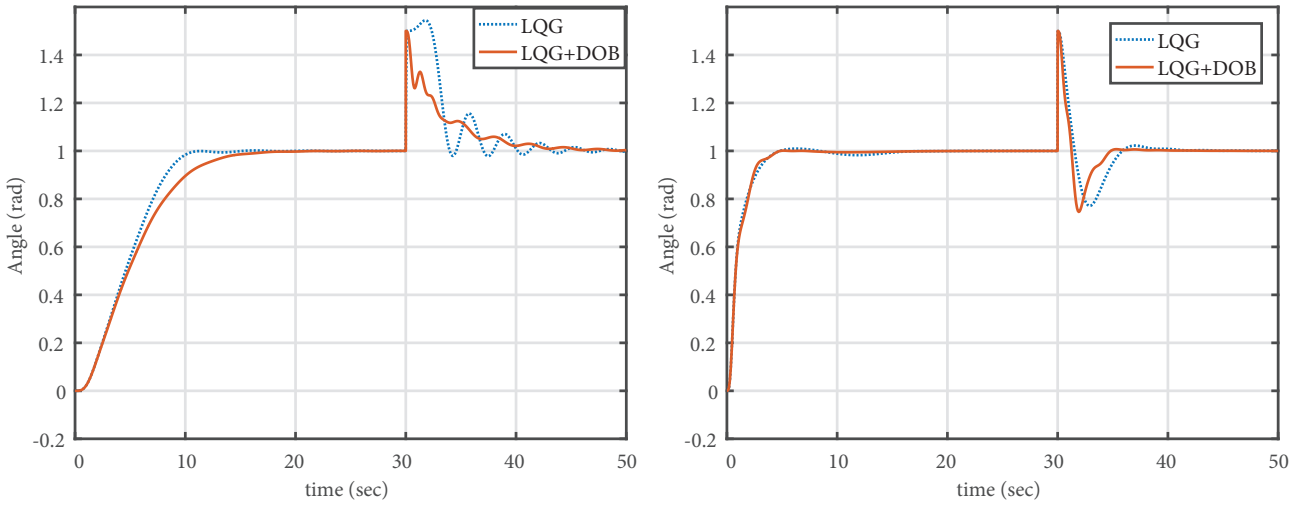

(a) main rotor (b) tail rotor

Figure 7. Response of TRAS for step input with step disturbance at t = 30 s.

Using LQG controller instead of PID as baseline feedback controller better response is obtained. For the main rotor the overshoot is minimized from 5% to 0% and smooth response is obtained with no fluctuations, whereas for tail rotor the settling time is reduced to 4.15 seconds from 10 seconds. The responses of PID, LQG, PID with DOB and LQG with DOB are compared in Figure 8a and 8b. The performance of proposed approach (LQG with DOB) for main and tail rotors is compared with other controllers in the literature in Table 3. Comparison shows that in addition to enhanced disturbance rejection capability the proposed approach (LQG with DOB) delivers better performance. Figure 9a shows the response of main and tail rotors of TRAS for square wave input where as Figure 9b shows the response of main and tail rotors of TRAS for sine wave input signal.

Table 3. Comparison of performance of proposed approach with other approaches in simulation.

	Main rotor		**Tail rotor**	
	Settling time	Peak overshoot	Settling time	Peak overshoot
SMC with NL SO [24]	40	0	10	0
BFO optimized PID [21]	10	5	13	4
LQG with DOB	14.1	0	4.15	0.11

The performance of DOB designed through H_∞ approach for the main rotor subsystem is analyzed in frequency domain as shown in Figure 10a, where D_{11} and D_{12} represents the DOB transfer functions $D_1(s)$

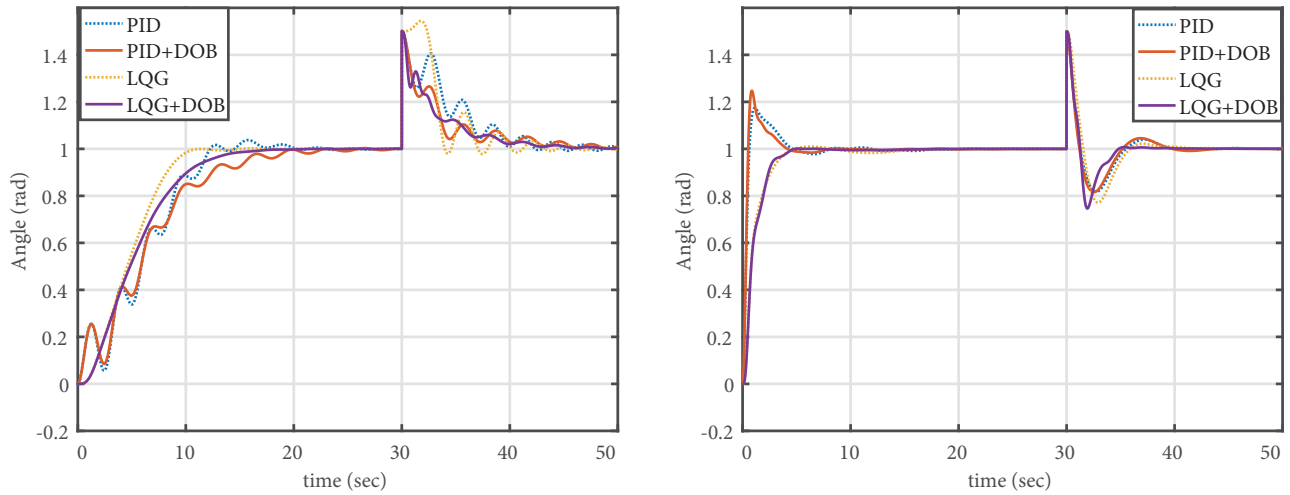

(a) main rotor (b) tail rotor

Figure 8. Response of TRAS for step input with step disturbance at t = 30 s.

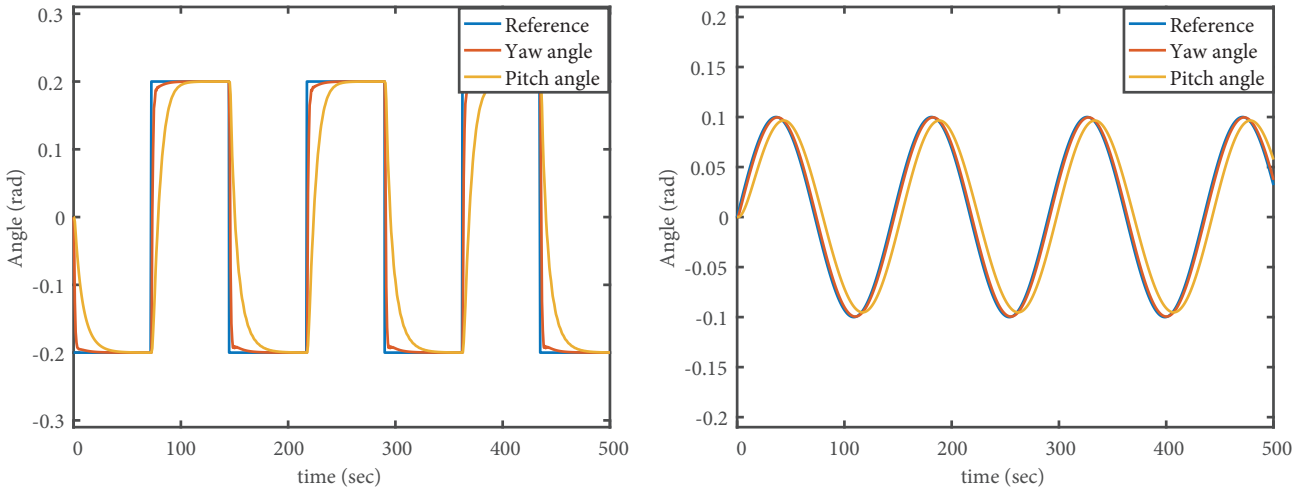

(a) Square wave response (b) Sine wave response

Figure 9. Square wave and sine wave response of TRAS

and $D_2(s)$, respectively, while G_m^{-1} represents the inverse of the main rotor subsystem's transfer function which is noncausal. From the bode plots it is observed that the reconstructed plant inverse $-D_1(s)^{-1}D_2(s)$ matches the noncausal nominal plant inverse very well over the frequencies up to 20 Hz. It is also seen $-D_2(s)$ approximates the behavior of low pass filter. Similarly the bode plots of DOB designed through H_∞ approach for the tail rotor subsystem is shown in Figure 10b. Here the reconstructed plant approximates the behavior of the noncausal and unstable nominal plant inverse over the frequencies up to 45 Hz.

7. Conclusion

In this paper, a laboratory helicopter model, also known as TRAS is decoupled into main and tail rotors subsystems. First, PID controllers are employed as outer loop feedback controllers for each subsystems to

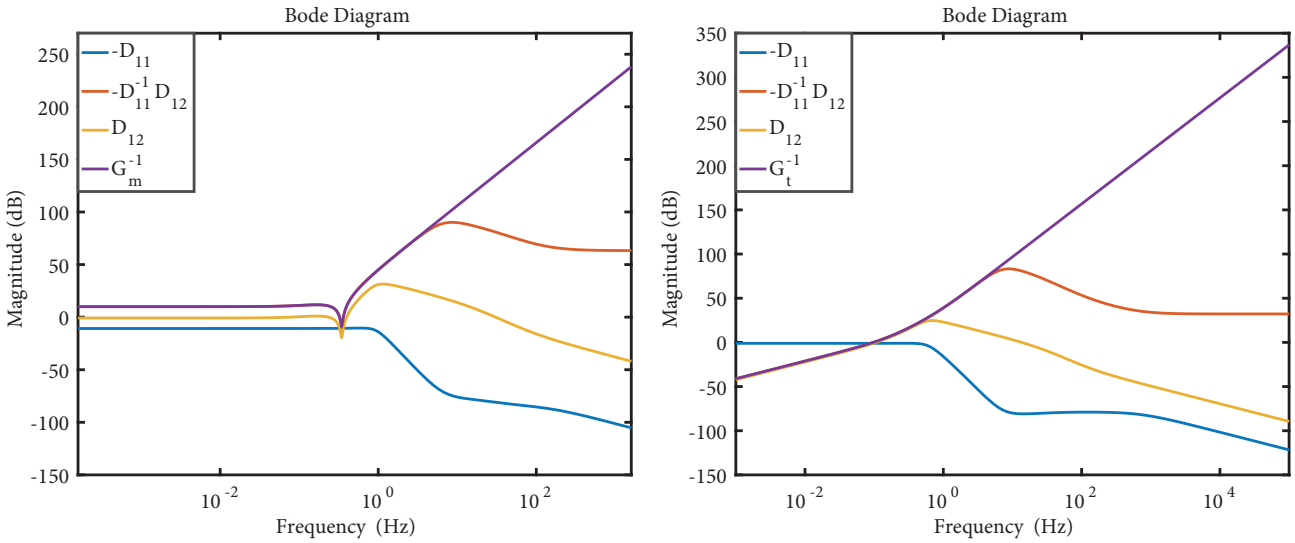

(a) main rotor (b) tail rotor

Figure 10. Bode diagram of the proposed H_∞ based DOB design for TRAS.

ensure stability and meet the performance specifications, and disturbance observers are designed for the inner loops to reject external disturbances. Then LQG controllers are designed and used as outer loop feedback controllers with DOBs. A systematic approach using H_∞ control theory is utilized for the design of disturbance observers. Simulations with nonlinear simulink model are performed and comparison is made between the closed loop systems with and without DOB. Comparisons show that in addition to enhanced disturbance rejection capability the proposed approach (using LQG with DOB) delivers better performance. Results also show that the 2 conflicting requirements, i.e. reference tracking and disturbance rejection, are met simultaneously by designing the outer loop feedback controller and the inner loop disturbance observer. In implementing the proposed techniques on a real plant, some performance degradation is to be expected as even a very elaborate nonlinear model would not be a 'true' representation of the plant. For that reason, performance measures like 2-norm and integral squared error (ISE) would be helpful for quantifying the difference between simulated and experimental responses.

References

[1] FANG Y, Shen H, SUN X, Zhang X, Xian B. Active disturbance rejection control for heading of unmanned helicopter. Control Theory and Applications 2014; 31 (2): 238-243.

[2] Chen M, Ge SS, How BV. Robust adaptive neural network control for a class of uncertain MIMO nonlinear systems with input nonlinearities. IEEE Transactions on Neural Networks 2010; 21 (5): 796-812.

[3] Juang JG, Huang MT, Liu WK. PID control using presearched genetic algorithms for a MIMO system. IEEE Transactions on Systems, Man, and Cybernetics, Part C (Applications and Reviews) 2008; 38 (5): 716-727.

[4] Ahmad M, Ali A, Choudhry MA. Fixed-Structure H_∞ Controller Design for Two-Rotor Aerodynamical System (TRAS). Arabian Journal for Science and Engineering 2016; 41 (9): 3619-3630.

[5] Ahmad U, Anjum W, Bukhari SM. H_2 and H_∞ controller design of twin rotor system (TRS). Intelligent Control and Automation 2013; 4 (1): 55-62.

[6] Nejjari F, Rotondo D, Puig V, Innocenti M. Quasi-LPV modelling and non-linear identification of a twin rotor system. In: IEEE 20th Mediterranean conference on control and automation (MED); Barcelona, Spain; 2012. pp. 229-234.

[7] Rahideh A, Shaheed MH. Hybrid fuzzy-PID-based control of a twin rotor MIMO system. In: IECON 2006-32nd Annual Conference on IEEE Industrial Electronics; Paris, France; 2006. pp. 48-53.

[8] Falb P, Wolovich W. Decoupling in the design and synthesis of multivariable control systems. IEEE transactions on automatic control 1967; 12 (6): 651-659.

[9] Ulasyar A, Zad HS. Robust and optimal model predictive controller design for twin rotor MIMO system. In: IEEE 9th International Conference on Electrical and Electronics Engineering; Bursa, Turkey; 2015. pp. 854-858.

[10] Duţescu DA, Radac MB, Precup RE. Model predictive control of a nonlinear laboratory twin rotor aero-dynamical system. In: IEEE 15th International Symposium on Applied Machine Intelligence and Informatics (SAMI); Herlany, Slovakia; 2017. pp. 000 037-000 042.

[11] Umeno T, Hori Y. Robust speed control of DC servomotors using modern two degrees-of-freedom controller design. IEEE Transactions on industrial electronics 1991; 38 (5): 363-368.

[12] Hoyle DJ, Hyde RA, Limebeer DJ. An h/sub infinity/approach to two degree of freedom design. In: Proceedings of the 30th IEEE Conference on Decision and Control; Brighton, England; 1991. pp. 1581-1585

[13] Fujimoto Y, Kawamura A. Robust servo-system based on two-degree-of-freedom control with sliding mode. IEEE Transactions on Industrial Electronics 1995; 42 (3): 272-280.

[14] Zeghlache S, Amardjia N. Real time implementation of non linear observer-based fuzzy sliding mode controller for a twin rotor multi-input multi-output system (TRMS). Optik-International Journal for Light and Electron Optics 2018; 156: 391-407.

[15] Rao VS, George VI, Kamath S, Shreesha C. Stability analysis of closed loop TRMS with observer based reliable H infinity controller using Kharitonov's stability theorem. International Journal of Engineering and Technology (UAE) 2018; 7 (2): 106-111.

[16] Mobayen S, Majd VJ, Sojoodi M. An LMI-based composite nonlinear feedback terminal sliding-mode controller design for disturbed MIMO systems. Mathematics and Computers in Simulation 2012; 85: 1-10.

[17] Flesch RC, Normey-Rico JE, Flesch CA. A unified anti-windup strategy for SISO discrete dead-time compensators. Control Engineering Practice 2017; 69: 50-60.

[18] Chen WH, Yang J, Guo L, Li S. Disturbance-observer-based control and related methods—an overview. IEEE Transactions on Industrial Electronics 2016; 63 (2): 1083-1095.

[19] Pradhan JK, Ghosh A. Design and implementation of decoupled compensation for a twin rotor multiple-input and multiple-output system. IET Control Theory & Applications 2013; 7 (2): 282-289.

[20] Twin Rotor MIMO System Control Experiments 33-949S User Manual. East Sussex, UK: Feedback Instruments Ltd, 2006.

[21] Pandey SK, Dey J, Banerjee S. Design of robust proportional–integral–derivative controller for generalized decoupled twin rotor multi-input-multi-output system with actuator non-linearity. Proceedings of the Institution of Mechanical Engineers, Part I: Journal of Systems and Control Engineering 2018; 232 (8): 971-982.

[22] Zheng M, Zhou S, Tomizuka M. A design methodology for disturbance observer with application to precision motion control: an H-infinity based approach. In: IEEE American Control Conference (ACC); Seattle, WA, USA; 2017. pp. 3524-3529.

[23] Lyu X, Zhou J, Gu H, Li Z, Shen S et al. Disturbance observer based hovering control of quadrotor tail-sitter VTOL UAVs using H_∞ synthesis. IEEE Robotics and Automation Letters 2018; 3 (4): 2910-2917.

[24] Saroj DK, Kar I, Pandey VK. Sliding mode controller design for Twin Rotor MIMO system with a nonlinear state observer. In: IEEE International Mutli-Conference on Automation, Computing, Communication, Control and Compressed Sensing (iMac4s); Kerala, India; 2013. pp. 668-673.